Composites: Part A 40 (2009) 60–66

Contents lists available at ScienceDirect

Composites: Part A

journal homepage: www.elsevier.com/locate/compositesa

Mechanical response of longleaf pine to variation in microfibril angle, chemistry associated wavelengths, density, and radial position

B.K. Via [a,*], C.L. So [b,c], T.F. Shupe [c], L.H. Groom [b], J. Wikaira [d]

[a] School of Forestry and Wildlife Sciences, Auburn University, AL 37067, USA
[b] Wood Products Utilization Research Unit, Pineville, LA 71360, USA
[c] LSU AgCenter, Baton Rouge, LA 70803, USA
[d] Wood Technology Research Centre, Christchurch, New Zealand

ARTICLE INFO

Article history:
Received 30 May 2008
Received in revised form 25 September 2008
Accepted 13 October 2008

Keywords:
A. Wood
B. Plastic deformation
C. Micro-mechanics
D. Mechanical testing

ABSTRACT

The composite structure of the S_2 layer in the wood cell wall is defined by the angle of the cellulose microfibrils and concentration of polymers and this structure impacts strength and stiffness. The objective of this study was to use near infrared spectroscopy and X-ray diffraction to determine the effect of lignin and cellulose associated wavelengths, microfibril angle, density, and radial position within the tree on strength and stiffness. The aromatic portion of lignin provided a good predictive role on strength and stiffness at high microfibril angles. However, in mature wood where microfibril angle and lignin content was low, cellulose associated wavelengths became increasingly important. The increased importance of the aromatic portion of lignin (1665 nm) on the strength as microfibril angle increased was attributable to the plastic deformation of lignin that occurred beyond the yield point. Finally, a fourfold increase in stiffness was observed when the microfibril angle dropped from 40 to 5°.

1. Introduction

At the macrolevel, wood itself is an orthotropic material that is inexpensive and acts as reinforcement for some more advanced composite products [1]. An understanding of the nanostructure of wood on the mechanical properties is thus critical. At the nanolevel, wood is a composite material composed of cellulose elementary fibers embedded in a hemicellulose and lignin matrix. Various models of the cross-section exist, but in general, the cellulose elementary fibers exhibit the least variation in dimension, probably due to its crystalline nature (3.5 × 3.5 nm) [2]. The hemicellulose matrix varies around 2.5 nm, is sandwiched between cellulose elementary fibers, and acts as a bridge between cellulose and the lignin [3,4]. The lignin polymer acts as a sheath around the cellulose and hemicellulose matrix, is sandwiched between other microfibers, and varies in content as a function of microfiber angle [3]. The lignin is entangled in xylan portion of the hemicelluloses while the glucomannan is associated directly with the microfibril [4–8].

Cellulose has been shown to dominate the elastic response when the load is applied nearly parallel to the cellulose plane, while lignin and hemicelluloses become more important as the angle of the load approaches the transverse direction where strength is greatly reduced by a factor of 10 at the nanoscale [9–14]. Based on these observations, it is conjectured that the importance of lignin on strength and stiffness should be higher in juvenile wood than mature wood. In juvenile wood, stresses in the lignin matrix is closer to the perpendicular plane of the polymer composite matrix as a result of the higher microfibril angle. Additionally, the stiffness of the material decreases in a non-linear manner with increased microfiber angle [3,15].

Since cellulose, hemicellulose, and lignin exhibit vastly different mechanical properties and they are connected together in and around the microfibrils, it is likely that shear forces will develop at the interface regions between polymer types. This was suggested as early as 1919 when slip planes was observed to develop parallel to the microfibrils [16]. Such planes occur since crystalline microfibrils act as a reinforcement mechanism resulting in shear forces at the interface [17]. Plastic deformation occurs in the lignin and hemicellusic matrix paralleling the cellulose polymer under such shear forces [18,19]. In order to prolong slip planes, such that deformation occurs at higher loads, the bonds from lignin to hemicelluloses needs to be adequate enough to transfer stress [20]. As noted earlier, for higher microfibril angles, loads parallel to the stem and tracheids (or fibers) occur closer to the plane that is perpendicular to the microfibrils resulting in compression of the lignin matrix. Such a plastic response was supported by Burgert et al. [21] where the modulus of rupture, was influenced by microfibril angle. It is probable that as microfibril angle increased [21], so did the shear stress between the lignin to hemicellulosic–cellulose matrix.

* Corresponding author. Tel.: +1 615 972 3666; fax: +1 334 844 4221.
E-mail address: bvia@hotmail.com (B.K. Via).

1359-835X/$ - see front matter © 2008 Published by Elsevier Ltd.
doi:10.1016/j.compositesa.2008.10.007

The elevated shear stress at higher microfibril angles resulted in permanent damage to the lignin structure. Likewise for the present study, it was hypothesized *a priori* that lignin played an increased role on the modulus of rupture in the juvenile wood region since microfibril angle is higher and the stress to strain curve exhibits more curvature, an indication of increased plasticity [22,23].

Finally, as a tree grows, significant longitudinal growth strains occur in the stem [24]. In order to prevent rupture from such growth development, the rheological behavior of the chemical constituents and the microfibril fibril angle in the cell wall become important. Kojima and Yamamoto show the longitudinal creep to increase with increasing microfibril angle [25]. Such behavior favors a rapidly growing stem whose large microfibril angle results in increased creep to counteract the considerable longitudinal growth stresses exhibited by the tree. Likewise, large microfibril angles are often coupled with higher lignin and lower cellulose which also favors increased potential for plastic deformation under long term loading [26].

The objective of this study was to investigate the role of cellulose, lignin, and hemicelluloses associated wavelengths, density, microfibril angle, and ring number on the modulus of rupture (MOR) and modulus of elasticity (MOE).

2. Materials and methods

2.1. Sample preparation

Ten longleaf pine (*Pinus palustris*) trees were harvested at a stand age of 41 years. Counting from the outer ring backward, the height of the tree reached breast height within 2–8 years. A range of diameters were chosen such that the lower 10th, mean, and upper 90th percentile in mean diameter was sampled. The site was managed at the Harrison Experimental Forest by the United States Forest Service in Saucier, Mississippi, U.S.A., at a location of 30.6° north and 89.1° west. Each tree was bucked every 4.57 m in height yielding five to seven disks. The number of disks was dependent on tree height. The disks were used to make bending specimens 30.48 cm × random width × 1.27 cm. The random width was a function of ring size and the ability to mill the specimen to ring size. When the ring size was quite small, often less than 1 mm in width, then the ring number of interest was placed as close to the neutral axis as possible.

From the remainder of the disk(s), the radial-longitudinal face was exposed for near infrared reflectance (NIR) spectra collection by cutting out 2 mm thick strips. Spectra were acquired at rings 2, 4, 8, 16, 32, and 40. We counted backwards from bark to pith such that the ring nearest the bark was ring 41 and the ring nearest the pith was ring 2. Due to the variability in time to reach a given height, sometimes rings 2 and 4 were not available for spectra collection. Ring 2 was only counted if the pith was present to validate that it was indeed ring 2. Rings with defects such as knots, cracks, and other unusual defects were removed from the analysis. There was no sign of blue stain on these trees, a variable which could impact spectra collection [27].

2.2. Mechanical testing

All specimens were conditioned to an equilibrium moisture content of 8% and with a coefficient of variation of 16.3%. The samples were weighed until gravimetric weight became constant. Loading was applied at a rate of 0.20 cm min^{-1} on the tangential longitudinal face in three-point bending set-up. The linear portion of the stress versus strain curve was used to calculate modulus of elasticity (MOE). Modulus of rupture (MOR), moisture content, and air dry density were determined by standard ASTM methods [28,29]. For the density measurement, the volume was measured by calipers to the nearest 0.0025 cm at 8% moisture content. Weights were measured to the nearest 0.001 g, also at 8% moisture content. Mechanical testing was equivalent to Via et al. [30]. Stress was calculated based on the dimensions of the wood sample cross-section.

2.3. Microfibril angle/T-value measurement

Small molecule X-ray crystallography was performed on a Bruker diffractomer. The *T*-value was used to estimate the sensitivity of mechanical properties to microfibril angle. The *T*-value is value closely related to the variance intensity of the (0 0 2) arc. Cave [31], along with personal communication, found *T*-value = MFA + 2SDA were SDA represents the standard deviation of the flank angle [3]. For this research, there was no need to translate from the *T*-value to MFA since they are so related, so the *T*-values were used to determine if MFA was statistically related to mechanical properties. However, Via et al. validated with microscopy the ability of the *T*-value to predict MFA for longleaf pine [3].

2.4. NIR spectroscopy

A scanning probe spectrometer (Nexus 670 FT-IR; Thermo Nicolet Instruments, Madison, WI, USA) was used to acquire the absorbance between 1000 and 2500 nm. An 8 mm spot size was the scan diameter. When the ring was smaller than the spot size, the ring was placed in the center of the scan area. Due to this measurement constraint, the spectra acquired from rings 30 and 40 were usually averages of several earlywood and latewood rings present within the circumference of the scan.

All scans were acquired at 1 nm intervals on the north and south side of the tree and then averaged. All scans were also taken on the radial-longitudinal face of the wood strips, which were cut on a band saw from the increment cores. During a single scan, a single spectrum was acquired as the average of 40 scans from the same spot. An intermediate software [32] was then used to transform the original spectra to the first derivative of absorbance before exporting the data to the statistical analysis software [33] for multivariate analysis. Prior to taking the 1st derivative, the spectrum was also averaged to 10 nm intervals in Unscrambler [32]. The reduction of the spectrum into 10 nm intervals has been shown to have no detrimental influence on model precision and performance [34]. A reference check was run every 10 min using a Spectralon standard (SRT-99-050, Labsphere, North Sutton, New Hampshire, USA).

2.5. Statistical analysis

Multiple linear regression was used to determine whether density, *T*-value (MFA associated), lignin, cellulose, and hemicellulose associated wavelengths were important in MOR and MOE variation. A literature review was performed a-priori to determine which wavelengths should associate with lignin, cellulose, and hemicellulose (Table 1). Then during the analysis stage, *t*-tests

Table 1
Assignment of absorption bands to important wood chemistry constituents.

Wavelength (nm)	Polymer/chemistry assignment	Reference
1130–1135	Aromatic portion of lignin	[43,46]
1423	Amorphous region of cellulose	[43]
1580	Crystalline region of cellulose	[43]
1672	Aromatic portion of lignin	[41–45]
1758	Alpha cellulose	[45]
1900	Lignin from foliar and branch material	[41]
2330	CH stretch in hemicellulose	[43]

were run to identify which wavelengths were statistically related to MOR and MOE. These statistically influential wavelengths were then compared to Table 1 to determine if lignin, cellulose, or hemicellulose were important in predicting MOR and MOE. Variables were determined to be significant at the $\alpha = 0.05$ level. Models were built for each ring number as well as across all ring numbers. The PROC REG procedure in SAS was used to compute *p*-values and build multiple regression models [33]. The R^2 was reported to estimate the percentage of variation that the independent variables contributed to MOR and MOE. The adjusted R^2 was reported to demonstrate when a potential overfit of the equations occur while the variance inflation factor (VIF) was used to ensure that the independent variables were not highly related, a common problem between wavelengths in the near infrared region [33]. A VIF < 3 was the constraint applied to determine if the covariance between wavelengths was acceptable to apply multiple linear regression [33].

Principal components were also computed from the absorbance at all wavelengths and then regressed against MOR and MOE [33]. Prior to computing principal components, the absorbance at each wavelength was standardized to a mean = 0 and a standard deviation = 1. The maximum adjusted R^2 was used to select those principal components that were statistically significant in predicting MOR and MOE [33]. The coefficients of the statistically significant principal components were then plotted across all wavelengths to determine which wavelengths were most influential to MOR and MOE. Wavelengths with the highest coefficients (±) (peaks and valleys) were then compared to Table 1 to determine if the wavelengths in Table 1 fell near the peaks and valleys; thus, principal components regression (PCR) was used to validate whether the wavelengths in Table 1 were important in predicting MOR and MOE.

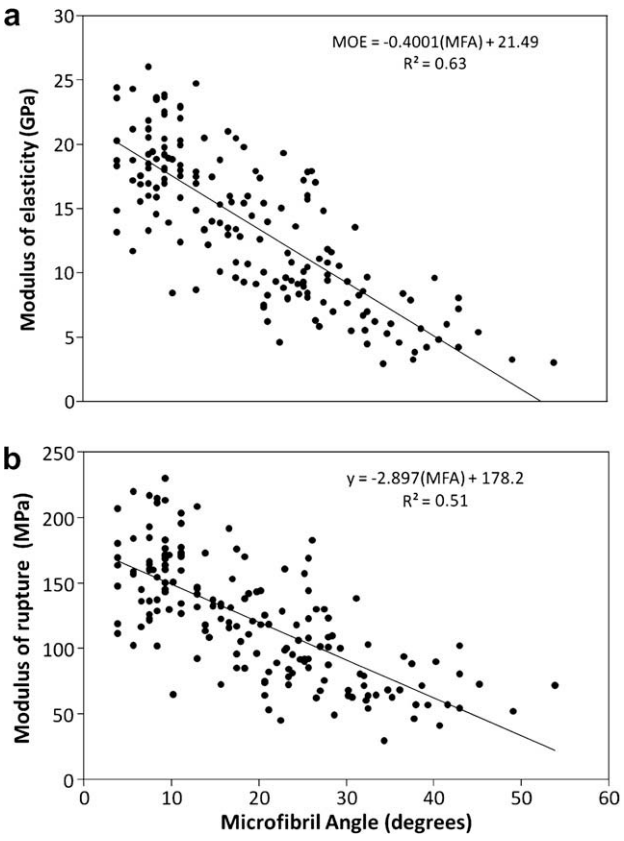

Fig. 1. MOE (a) and MOR (b) response to microfibril angle across all ring number and heights.

3. Results and discussion

3.1. Whole tree strength and stiffness versus microfibril angle

Fig. 1a and b demonstrate the effect of MFA on MOR and MOE across an aggregate of ring numbers and tree heights. A linear regression model was fit to the data to estimate the slopes. Prior to the study, a non-linear relationship between MFA and MOE was anticipated since experimental data from the S_2 layer supported the longitudinal elastic modulus to be non-linear [10,35,36]. Yang and Evans decided to handle the non-linear behavior by dividing density by MFA ($R^2 = 0.92$) [37]. The same transformation procedure worked for *E. delegatensis* with an $R^2 = 0.94$ between longitudinal modulus of elasticity and density/MFA [38]. However, when we tried to divide density by MFA for this data set, there was no such relationship, an indication that this transformation procedure may be species specific. Additionally, we analyzed a family of non-linear curves and the exponential fit ($R^2 = 0.66$) was the best performing but still performed similarly to a linear fit ($R^2 = 0.63$). Since the slopes for exponential and linear fits were very similar for the entire range of microfibril angles, we chose to assume linearity for statistical testing.

According to Fig. 1a, when linearity was assumed, there was approximately a fourfold increase in stiffness when going from 40 to 5°. This nearly compares with Cave and Walker who found a fivefold increase in stiffness when going from juvenile to mature wood for *Pinus radiata* [35].

The threefold increase in MOR with decreased MFA (40 to 5°) was especially interesting. Conventionally, the largest contribution of microfibril angle has been to stiffness and not strength. But more recently, attention has been given to the interaction between MFA and matrix yield beyond the proportional limit. The viscoelastic response on the non-linear portion of the stress–strain curve can be attributed to slippage of microfibrils past one another, coupled with plastic deformation within the microfibular matrix [39]. Burgert et al. found the microfibril angle to play a pivotal role in stiffness below the proportional limit and yield beyond the proportional limit [21]. Such relationships occurred despite partial reorientation of microfibrils coupled with plastic deformation. It was likely these potential interactions at the nanolevel were responsable for the apparent relationship between MOE and MOR at the macro level as seen in our data. Fig. 2 demonstrates the very strong relationship that occurred between MOR and MOE. In addition to the possible covariance between microfibril angle, strength, and stiffness at the nanolevel, it was probable that density, strength, and stiffness covariance at the macro level also

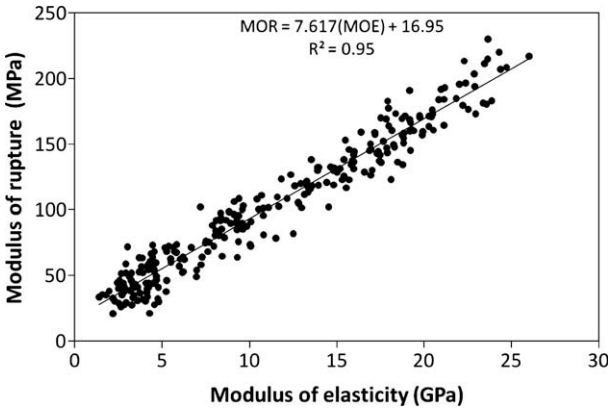

Fig. 2. The response of MOR to MOE across all ring number and heights.

added to the tight covariance between MOR and MOE (Fig. 2). On the other hand, the anisotropic nature of wood will often dominate the failure mode and mask any impact due to microfibril angle or other wood polymer concentration. It should thus be noted that for this experiment, extreme ranges in microfibril angle, wood chemistry, and wood density were selected which in turn optimized their influence on MOR and MOE.

3.2. Effect of whole tree density, polymer angle, and chemistry on strength and stiffness

Recently, near infrared spectroscopy has become useful in accessing variation in wood chemistry associated wavelengths [40]. In that paper, several investigators were referenced for their assignment of wood chemistry to specific wavelengths in the near infrared range [41–46]. In this study, these same wavelengths were used to investigate the sensitivity of strength and stiffness to lignin, cellulose, and hemicelluloses associated wavelengths (Table 1).

Table 2 summarizes the effect of MFA, density, and chemistry associated wavelengths with MOR and MOE for all ring numbers. Using the backward selection procedure in PROC REG [33], the exact same four variables were needed for predicting MOE as MOR. These results support that for longleaf pine, the slope of the stress strain curve was highly related to the final rupture point. The similarity between MFA, density, 1675, and 1765 nm associated wavelengths and its effects on MOR and MOE may partially help to explain why MOR and MOE was correlated (Fig. 2). In Fig. 1, the relationship between final rupture point and elastic response may be partially attributable to microfibril orientation and its interaction with the lignin matrix. As the microfibril angle increases, the shear stresses in the lignin matrix should rise which in turn result in higher plastic deformation in the lignin matrix. Burgert et al. [21] noticed a relationship between MFA and plastic response despite significant cell wall deformation. For our study, as microfibril angle increased, the MOR decreased, and the lignin associated wavelength (1665 nm) exhibited a significant peak. The distinct peak at 1665 nm for the low MOR group in Fig. 3b was evidence of the plastic deformation that occurs in the lignin matrix past the yield point. As one might expect, when the stress strain curve remained in the elastic region, the impact of the 1665 nm wavelength was much less pronounced (Fig. 3a).

In addition to multiple linear regression, principal components regression was performed to validate if the wavelengths chosen in Table 1 were indeed those needed for hypothesis testing in Table 2. Principal components 1, 3, 4, 5, 6, and 8 were important in predicting MOE ($R^2 = 0.75$). Principal components 1, 3, 4, 5, and 6 were important in predicting MOR ($R^2 = 0.79$). Principal components regression also supported the fact that the same underlying chemistry variables needed to predict MOR were also needed to predict MOE.

Fig. 4a, b, and c represent the coefficients at different wavelengths for principal components 4, 5, and 6. All three of these components were important in predicting both MOR and MOE (p-value < 0.05). The highest absolute value on the chart (global peaks and valleys) represent those wavelengths most influential in defining the principal component and hence have a stronger impact on MOR and MOE. Principal component 4 demonstrated that alpha cellulose (1758 nm) was very important in predicting MOR and MOE. Principal component 5 accounted for lignin and hemicelluloses associated wavelengths as per Tables 1 and 2 (Fig. 4b).

Table 2
Multiple linear modeling significance testing for MFA, density, and chemistry associated wavelengths (1st derivative): combined and partitioned by ring number.

Mechanical property	Ring number	Independent variable	p-Value	R^2	Adjusted R^2	Sample size
MOE & MOR	All	MFA Density 1675 1765	*** *** *** ***	0.9 & 0.86	0.89 & 0.85	162
MOE	4	MFA 1675	*** **	0.61	0.35	47
MOR	4	MFA	*	0.49	0.35	47
MOE	8	MFA Density 1675	*** ** **	0.76	0.69	50
MOR	8	MFA Density 1675	** ** *	0.61	0.52	50
MOE	16	Density 1155 1605 1675 1765	** * * ** **	0.81	0.75	45
MOR	16	Density 1605 1765	** * **	0.77	0.71	45
MOE	29	MFA Density	** *	0.83	0.55	16
MOR	29	MFA Density 1155 1605 1895	** * * ** **	0.92	0.78	16

A *, **, and *** represents a p-value of <0.05, <0.01, and <0.001, respectively.

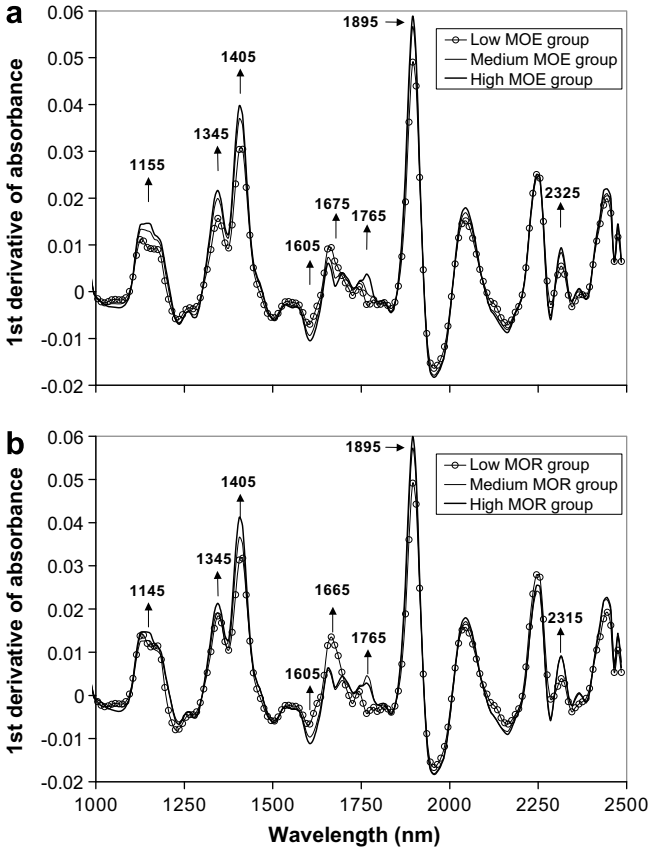

Fig. 3. The response of the first derivative of absorbance to low, medium, and high MOE (a) and MOR (b). Potential discriminatory wavelengths are labeled and marked with arrows.

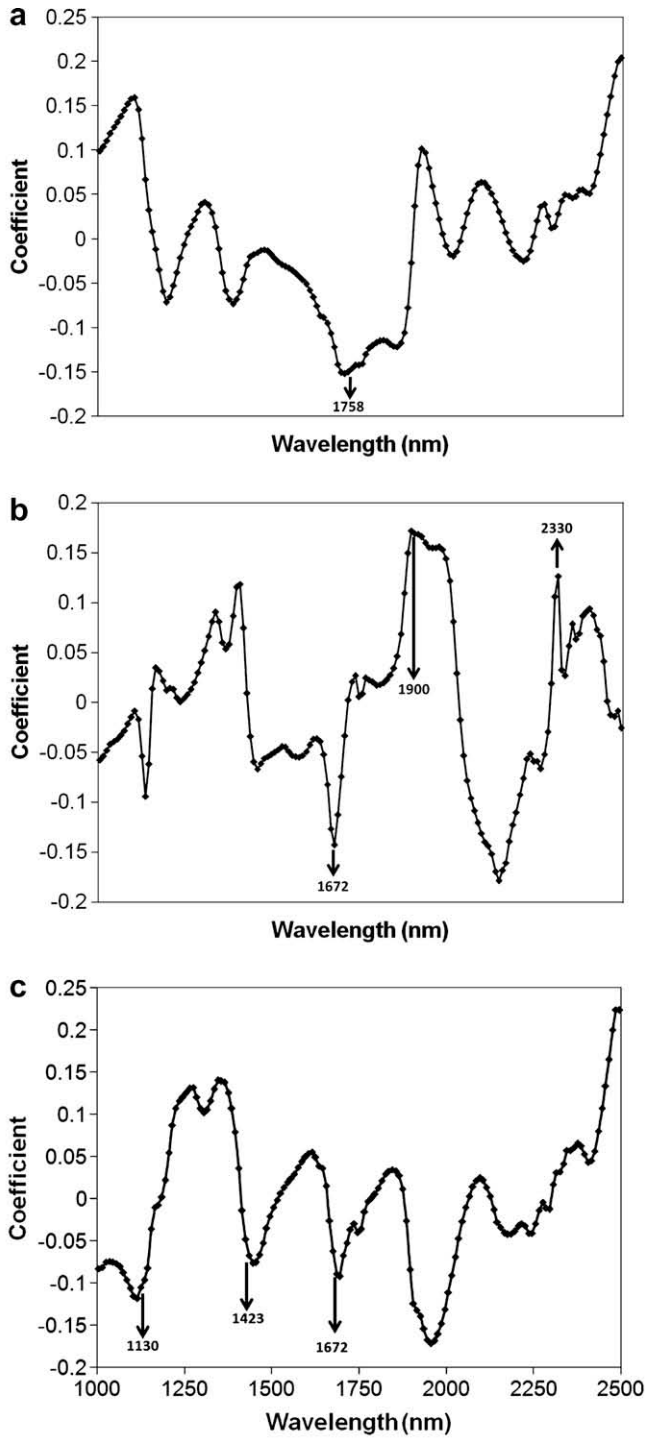

Fig. 4. Coefficients for statistically significant principal components in predicting MOR and MOE. Principal component 4 (a) principal component 5 (b) and principal component 6 (c) were some of the factors important in predicting MOR (R^2 = 0.79) and MOE (R^2 = 0.75). Discriminatory wavelengths chosen *a priori* are labeled and marked with arrows.

What was interesting was that the hemicellulose associated wavelength emerged as being important for MOR and MOE when using principal components regression. However, when multiple linear regression was used (Table 2), hemicellulose signals were not able to be detected due to extremely high multicollinearity with other wavelengths. Finally, principal component 6 accounted for two wavelengths associated with the aromatic portion of lignin and the amorphous region of cellulose (Fig. 4c and Table 1).

3.3. Partitioning of effects on MOR and MOE by ring number

Table 2 summarizes the effect of MFA, density, and chemistry associated wavelengths on MOR (and MOE) at different ring numbers. At rings 4 through 16, the majority of which would be considered juvenile wood, MFA and lignin associated wavelengths (1675 nm) were predominant in predicting MOR while density was also important, but to a lesser extent. However, at rings 16 and 29, density and MFA exhibited an equal effect with density on MOR exhibiting a statistical edge at ring 16. Conversely, at ring 29, MFA statistically edged out density when predicting MOR; however, it took five variables to predict MOR with a sample size of only 16. As a result, care should be taken when interpreting ring 29. When rings 16 and 29 were analyzed together, not shown in Table 2, density was more influential on MOR than MFA. The alpha cellulose associated wavelength (1765 nm) was not influential on MOR in rings 4 and 8 but was important at ring 16. For ring 29, the 1605 nm peak was important and may be attributable to the crystalline region of cellulose (1580 nm – Table 2). It was assumed that the 1580 nm peak (crystalline region of cellulose) shifted slightly to our average of 1605 nm. This shift to higher wavelengths was also observed at 1135 nm, indicative of machine differences between our study and the data obtained in Table 2. For our study, the influence of cellulose associated wavelengths on MOR for lower microfibril angles agreed with Eichhorn et al. [9] who found cellulose associated wavelengths to shift during deformation while lignin associated wavelengths did not.

In summary, lignin and MFA was more important in predicting MOR in the juvenile portions of the tree while cellulose became more important in the mature regions. The hemicellulose associciated wavelength (2330 nm) was not found to be influential on MOR. However, it is probable that the variation explained by hemicellulose could also be explained by the variation in cellulose and lignin since the sum of the three components commonly exceed 95% of the total weight for southern pine. This was supported by Winandy and Lebow [47] who found a high multicollinearity between chemical constituents within southern pine which is important because if the multicollinearity is too high, it can make it hard to rank variables using multiple linear regression analysis. Finally, in this study, even after taking the first derivative, there was still some multicollinearity present between absorbance at different wavelengths when the variance inflation factor was observed [47] and SAS was used to compute [33]. While the equations chosen in Table 2 had low VIF factors, some possible equations that included hemicellulose associated wavelengths did have a high VIF. As such, one can not conclude from this analysis that hemicellulose did not play an important role on MOR (or MOE). It is instead likely that the multicollinearity between chemical composition masked the effect of hemicellulose on MOR and MOE. Additionally, calibrations for hemicellulose from NIR spectra are quite low compared to cellulose and lignin which is likely to bias our analysis toward cellulose and lignin as being more influential [46].

Given that MOR and MOE were highly correlated (Fig. 2) it may be hypothesized that the underlying wood chemistry was partly responsible for the response in MOR and MOE. According to Table 2, this was the case with MFA and lignin associated wavelengths (1675 nm) being more influential on MOE at rings 4 and 8, while cellulose associated wavelengths became more important at higher ring numbers (Table 2). However, what was interesting was that the lignin associated wavelength (1675 nm) exhibited more variation between MOR classes (Fig. 3b) than MOE classes (Fig. 3a). This may be explained by

the fact that lignin exhibits plastic deformation past the proportional limit when loading to rupture. Such evidence was supported by Reiterer et al. [36] who believed that hemicellulose and lignin exhibits more plastic deformation when loaded at large angles to the polymer matrix axis. Since high MFA's and high lignin contents are present in juvenile wood (rings 4 and 8) and were highly influential on MOR (Table 2), this study supports others [3,36]. Likewise, Hepworth and Vincent [48], hypothesize that increasing MFA will result in compression forces that compact the amorphous region of lignin. Gindl et al. [49] concur and used nanoindentation to conclude that cellulose was important for stiffness while hemicellulose and lignin was more important for plastic deformation. Burgert et al. [21] add that MFA plays an important role both above and below the proportional limit and therefore is also important on MOR and MOE.

One important constraint in this study was that our samples were equilibrated to 8% moisture content with minimal variation. Such control of moisture content was necessary to improve the signal to noise ratio across a significant portion of the NIR spectrum [50,51]. However, in plant tissues, lignin exhibits less of an effect on strength at lower moistures due to the hydrophobicity of lignin [39]. Conversely, in the tree, the moisture content will be greater than fiber saturation making lignin more important beyond the linear elastic range because of its hydrophobicity [39]. As a result, this study was not able to account for the interaction between lignin and moisture on MOR or MOE and may have underestimated the impact of lignin for a given ring number. Nevertheless, given the agreement with this study to many others as found above, it was concluded that such an interaction effect on MOR or MOE, along with any bias, is probably minimal.

4. Conclusions

In conclusion, visual and statistical analysis of the 1st derivative of NIR absorbance for all ring numbers found the aromatic portion of lignin (1665–1675 nm) to be more important to MOR than MOE. When partitioned by ring, MFA and lignin associated wavelengths were more influential on MOE and MOR in the juvenile wood zone; while, in the transition (ring 16) and mature wood region (ring 29), cellulose associated wavelengths became increasingly important. Such a trend supports the hypothesis that the plastic response of lignin during loading is more prevalent when the matrix is loaded closer in the plane perpendicular (occurs with a high MFA) while cellulose becomes increasingly important when the polymer matrix is loaded closer to parallel (occurs with a low MFA). Likewise, the relationship between microfibril angle and stiffness agreed with other researchers for other tree species.

Acknowledgements

This paper (No. 2007-290-1225) is published with the approval of the Director of the Louisiana Agricultural Experiment Station. This study was funded by the USDA National Research Initiative Competitive Grants Program Agreement No. 2001-35103-10908. All data collection was performed either at Louisiana State University AgCenter or the USDA Forest Service in Pineville, Louisiana. The trees for this study were harvested and supplied by James Roberds and Larry Lott of the Southern Institute of Forest Genetics Southern Research Station, U.S. Forest Service.

References

[1] Espert A, Francisco V, Karlsson S. Comparison of water absorption in natural cellulosic fibers from wood and one-year crops in polypropylene composites and its influence on their mechanical properties. Composites: Part A 2004;35:1267–76.
[2] Nieduszy I, Preston RD. Crystallite size in natural cellulose. Nature 1970;225:273–4.
[3] Via BK, So C, Groom LH, Shupe TF, Stine M, Wikaira J. Within tree variation of lignin, extractives, and microfibril angle coupled with the theoretical and near infrared modeling of microfibril angle. IAWA J 2007;28:189–209.
[4] Fengel D. Ultrastructural behavior of cell wall polysaccharides. Tappi J 1970;53:497–503.
[5] Adler E. Lignin chemistry–past, present, and future. Wood Sci Technol 1977;11:169–218.
[6] Yamamoto H, Kojima Y, Okuyama T, Abasolo WP, Gril J. Origin of the biomechanical properties of wood related to the fine structure of the multi-layered cell wall. Trans ASME 2002;124:432–40.
[7] Fromm J, Rockel B, Lautner S, Windeisen E, Wanner G. Lignin distribution in wood cell walls determined by TEM and backscattered SEM techniques. J Struct Biol 2003;143:77–84.
[8] Singh AP, Daniel G. The S2 layer in the tracheid walls of Picea abies wood: inhomogeneity in lignin distribution and cell wall microstructure. Holzforschung 2001;55:373–8.
[9] Eichhorn SJ, Sirichaisit J, Young RJ. Deformation mechanisms in cellulose fibres, paper and wood. J Mater Sci 2001;36:3129–35.
[10] Bergander A, Salmén L. Cell wall properties and their effects on the mechanical properties of fibers. J Mater Sci Lett 2002;37:151–6.
[11] Astley OM, Chanliaud E, Donald AM, Gidley MJ. Tensile deformation of bacterial cellulose composites. Int J Biol Macromol 2003;32:28–35.
[12] Barnett JR, Bonham VA. Cellulose microfibril angle in the cell wall of wood fibers. Biol Rev 2004;79:461–72.
[13] Gindl W, Schöberl T. The significance of elastic modulus of wood cell walls obtained from nanoindentation measurements. Composites: Part A 2004;35:1345–9.
[14] Salmén L. Micromechanical understanding of the cell-wall structure. C R Biol 2004;327:873–80.
[15] Tze WTY, Wang S, Rials TG, Pharr GM, Kelly SS. Nanoindentation of wood cell walls: continuous stiffness and hardness measurements. Composites: Part A 2007;38:945–53.
[16] Lang WH. The microscopical features of mechanical strains in timber and the bearing of these on the structure of the cell-wall in plants. J Philos Trans Roy Soc Lon B 1919;210:49–82.
[17] Jeronimidis G. The fracture behaviour of wood and the relations between toughness and morphology. Proc Roy Soc Lon B Biol Sci 1980;208:447–60.
[18] Taiz L. Plant cell expansion: regulation of cell wall mechanical properties. Ann Rev Plant Physiol 1984;35:585–657.
[19] Lucas PW, Darvell BW, Lee PK, Yuen TD, Choong MF. The toughness of plant cell walls. Philos Trans Biol Sci 1995;348:363–72.
[20] Cowdrey DR, Preston RD. Elasticity and microfibrillar angle in the wood of sitka spruce. Proc Roy Soc Lon B Biol Sci 1966;166:245–72.
[21] Burgert I, Frühmann K, Keckes J, Fratzl P, Stanzl-Tschegg S. Structure-function relationships of four compression wood types: micromechanical properties at the tissue and fibre level. Trees 2004;18:480–5.
[22] Groom L, Mott L, Shaler S. Mechanical properties of individual southern pine fibers. Part I. Determination and variability of stress–strain curves with respect to tree height and juvenility. Wood Fiber Sci 2002;34:14–27.
[23] Shupe TF, Choong ET, Stokke DD, Gibson MD. Variation in cell dimensions and fibril angle for two even-aged loblolly pine plantations. Wood Fiber Sci 1996;28:268–75.
[24] Gartner B. Trees have higher longitudinal growth strains in their stems than in their roots. Int J Plant Sci 1997;158:418–23.
[25] Kojima Y, Yamamoto H. Effect of microfibril angle on the longitudinal tensile creep behavior of wood. J Wood Sci 2004;50:301–6.
[26] Hori R, Suzuki H, Kamiyama T, Sugiyama J. Variation of microfibril angles and chemical composition: implications for functional properties. J Mater Sci Lett 2003;22:963–6.
[27] Via BK, Eckhardt LG, So C, Shupe TF, Groom LH, Stine M. The response of visible/near infrared absorbance to wood-staining fungi. Wood Fiber Sci 2006;38:717–26.
[28] American Society for Testing Materials. Standard methods of testing small clear specimens of timber: ASTM D 143-83, Philadelphia, PA, USA; 1993.
[29] American Society for Testing Materials. Standard test methods for specific gravity of wood and wood-base materials: ASTM D 2395-83, Philadelphia, PA, USA; 1993.
[30] Via BK, Shupe TF, Groom LF, Stine M, So CL. Multivariate modelling of density, strength, and stiffness from near infared for mature, juvenile, and pith wood of longleaf pine (Pinus Palustris). J Near Infrared Spectrosc 2003;11:365–78.
[31] Cave I. Theory of X-ray diffraction method for the measurement of microfibril angle in wood. For Prod J 1966;16:37–42.
[32] Unscrambler. Camo: version 7.5, Vika, Norway; 1999.
[33] Statistical Analysis Software. version 9.0, Cary, North Carolina, USA; 2002.
[34] Schimleck LR, Stürzenbecher R, Jones PD, Evans R. Development of wood property calibrations using near infrared spectra having different spectral resolutions. J Near Infrared Spectrosc 2004;12:55–61.
[35] Cave ID, Walker JCF. Stiffness of wood in fast-grown plantation softwoods: the influence of microfibril angle. For Prod J 1994;44:43–8.
[36] Reiterer A, Lichtenegger H, Tschegg S, Fratzl P. Experimental evidence for a mechanical function of the cellulose microfibril angle in wood cell walls. Phil Mag A 1999;79:2173–84.

[37] Yang JL, Evans R. Prediction of MOE of eucalypt wood from microfibril angle and density. Holz als Roh- und Werkstoff 2003;61:449–52.
[38] Evans R, Ilic J. Rapid prediction of wood stiffness from microfibril angle and density. For Prod J 2001;51:53–7.
[39] Köhler L, Spatz H. Micromechanics of plant tissues beyond the linear-elastic range. Plants 2002;215:33–40.
[40] Via BK, So C, Eckhardt LG, Shupe TF, Groom LH, Stine M. Response of diffuse reflectance spectra to blue stain and wood age. J. Near Infrared Spectrosc 2008;16:71–4.
[41] Soukupová J, Rock BN, Albrechtová J. Spectral characteristics of lignin and soluble phenolics in the near infrared–a comparative study. Int J Remote Sensing 2002;23:3039–55.
[42] Schwanninger M, Hinterstoisser B, Gradinger C, Messner K, Fackler K. Examination of spruce wood biodegraded by Ceriporiopsis subvermispora using near and mid infrared spectroscopy. J Near Infrared Spectrosc 2004;12:397–409.
[43] Tsuchikawa S, Inoue K, Mitsui K. Spectroscopic monitoring of wood characteristics variation by light-irradiation. For Prod J 2004;54:71–6.
[44] Yeh T, Chang H, Kadla JF. Rapid prediction of solid wood lignin content using transmittance near-infrared spectroscopy. J Agr Food Chem 2004;52:1435–9.
[45] Terdwongworakul A, Punsuwan V, Thanapase W, Tsuchikawa S. Rapid assessment of wood chemical properties and pulp yield of Eucalpytus camaldulensis in Thailand tree plantations by near infrared spectroscopy for improving wood selection for high quality pulp. J Wood Sci 2005;51:167–71.
[46] Jones DP, Schimleck LR, Peter GF, Daniel RF, Clark A. Nondestructive estimation of wood chemical composition of sections of radial wood strips by diffuse reflectance near infrared spectroscopy. Wood Sci Technol 2006;40:709–20.
[47] Winandy JE, Lebow PK. Modeling strength loss in wood by chemical composition Part I. An individual component model for southern pine. Wood Fiber Sci 2001;33:239–54.
[48] Hepworth DG, Vincent JF. Modelling the mechanical properties of xylem tissue from tobacco plants (Nicotiana tabacum 'Samsun') by considering the importance of molecular and micromechanisms. Ann Bot 1998;81:761–70.
[49] Gindl W, Gupta HS, Schöberl T, Lichtenegger HC, Fratzl P. Mechanical properties of spruce wood cell walls by nanoindentation. Appl Phys 2004;79:2069–73.
[50] Law DP, Trachuk R. Determination of moisture content in wheat by near-infrared diffuse reflectance spectrophotometry. Cereal Chem 1977;54:874–81.
[51] Gillon D, Dauriac F, Deshayes M, Valette JC, Moro C. Estimation of moisture content using near infrared reflectance spectroscopy. Ag For Meterol 2004;124:51–62.